Structural Durability & Health Monitoring

Tech Science Press

https://doi.org/10.32604/sdhm.2026.076141

ARTICLE

The Performance of Reinforced Concrete Tunnel Linings, with and without Fibers, after Twenty Years of Service

Mustapha Hatoum[1], **Alessandro P. Fantilli**[1,*], **Bernardino Chiaia**[1] **and Georgios Kalamaras**[2]

[1]Departement of Structural, Building, and Geotechnical Engineering/Politecnico di Torino, Torino, Italy
[2]AK Ingegneria Geotecnica Srl, Torino, Italy

*Corresponding Author: Alessandro P. Fantilli. Email: alessandro.fantilli@polito.it

Received: 14 November 2025; Accepted: 06 February 2026; Published: 18 May 2026

ABSTRACT: This study investigates the contribution of fibers to the durability of reinforced concrete tunnel linings. Two cast-*in-situ* tunnels are herein analyzed after twenty years of service. Tunnel #1, made with plain concrete and steel rebar, has shown significant spalling at joints between two consecutive tunnel panels, caused by poor workmanship and construction details. Conversely, in Tunnel #2, close to Tunnel #1 on the same motorway, fiber-reinforced concrete (FRC) was used in combination with steel rebar. During the service life, the amount of FRC spalled from the cold joints of this lining has been significantly lower than the volume of concrete detached in Tunnel #1, despite the presence of the same type of joint. Thus, the addition of steel fibers to concrete mixtures can increase the material toughness, which in turn reduces concrete spalling. Hence, fiber-reinforcement enhances not only the durability but also the resilience of tunnel linings (i.e., Tunnel #2). Consequently, FRC represents a sustainable solution to extend the service life of structures, and to reduce the costs associated with the maintenance and renovation of tunnel linings.

KEYWORDS: Compressive strength; flexural strength; yield strength; minimum reinforcement; cold joints; concrete spalling; maintenance and repairing costs

1 Introduction

In the design and construction of tunnels, practitioners face significant challenges, particularly when ensuring long-term durability and structural integrity [1]. Indeed, concrete tunnels can show different types of failures during their service life, which can be due to a combination of geotechnical, structural, and environmental factors.

Ground movement or settlement can cause considerable damage in the linings, especially in urban areas, where tunnels either interact with surrounding buildings and infrastructures or uncertain external terrain pressure is present [2].

High localized stress concentrations due to non-uniform surrounding actions, in addition to concrete shrinkage and thermal stresses, produce a cracking phenomenon, especially in the case of cast *in-situ* tunnels (see Fig. 1a) [3]. A diffuse crack pattern fosters water infiltration, which usually leads to reinforcement corrosion, if present (Fig. 1b), and lining deterioration [4]. Water infiltration typically occurs when concrete finishing and impermeabilization do not meet the design requirements. Moreover, in cast *in-situ* tunnel, poor workmanship usually generates construction problems, such as insufficient concrete cover, presence of honeycombs, and rapture or scratches in the impermeable membrane [5]. For these tunnels, the most common structural problems are the deterioration of concrete and heavy spalling. It consists of the breaking

of concrete fragments at a level that can compromise the structural integrity and the safety of the concrete linings as well [6].

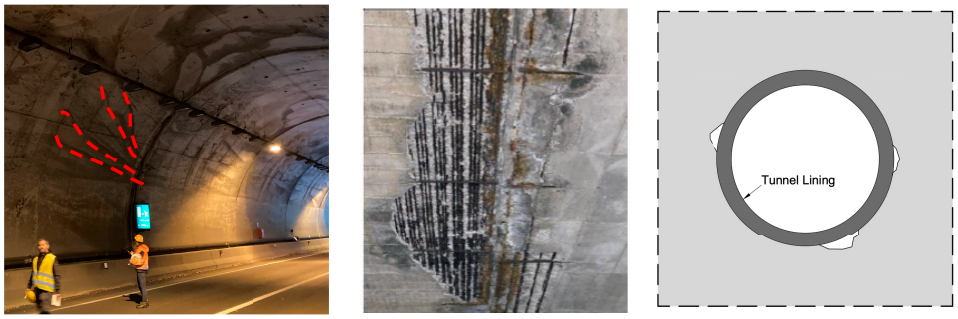

(**a**) (**b**) (**c**)

Figure 1: (**a**) Typical crack pattern in tunnels; (**b**) Spalling of concrete due to steel corrosion; (**c**) Erosion voids phenomenon around tunnel linings.

Typically, the spalling of concrete occurs at the interface between successive concrete pours (cold joint). It can lead to structural damage over time and requires high costs for repairing and maintenance [2], including the tunnel traffic closure. At damaged cold joints, water infiltration takes out soil and causes erosion and voids in the extrados of the lining, especially in buried infrastructure. As a result, the soil stresses around the extrados of the liner become unfavorable and may modify the internal actions in lining cross-sections [7]. This problem generally occurs in the case of tunnels surrounded by soft soil (Fig. 1c).

The use of durable materials and innovative construction techniques, such as fiber-reinforced concrete (FRC), can be a way to reduce the spalling failure and to enhance the long-term performance [8]. FRC is a cement-based composite that incorporates fibrous materials, such as steel, glass, polymeric, or natural fibers. The primary purpose of adding fibers is to improve the material properties, such as tensile toughness, which in turn affects in a direct positive way the durability [1]. The use of fibers in concrete started back in the early 20th century, but they have been used significantly since the 1970s with the development of steel and synthetic fibers [8]. Today, FRC is widely applied in two-way structures, especially in tunnel linings and concrete pavements [9].

In the case of tunnels excavated using the so-called tunnel boring machine (TBM), precast FRC segments forming the tunnel ring are the most common alternative to the traditional RC elements. Indeed, since the early 21st Century, contractors have started to accept more FRC than plain concrete, because the percentage of ordinary steel rebar can be reduced, and both crack control and post-cracking stiffness improve [10]. Fiber reinforcement is also performing well around the joints between the rings, where cracks produced by unforeseen soil actions or concentrated rock stresses are more likely to be generated [11].

FRC technology has also been used in cast-*in-situ* tunnels, when the mechanized excavation is not a feasible solution. In these cases, hybrid reinforcement (i.e., reinforced fiber-reinforced concrete R/FRC) appears to be a convenient solution when the amount of rebar can be reduced. This is particularly true in cross-sections subjected to bending moment and normal compression loads [12], like those of tunnel linings, where only the minimum reinforcement is needed [8]. Although hybrid reinforcement can avoid brittle failure and control crack width, studies concerning the durability of R/FRC linings are not very well documented in technical literature.

Accordingly, this paper presents a case study of two tunnels—Tunnel #1 and Tunnel #2—constructed in 2005 for the Turin Winter Olympics (Italy), having conventional cast-*in-situ* RC (mainly in the Tunnel #1) and

R/FRC (mainly in the Tunnel #2) linings. In the latter case, the use of fibers minimized the need for traditional rebar and reduced the time of construction [8], even if the long-term performance (i.e., durability) was not considered. Thus, in the next sections, after illustrating the original design procedure, the current health condition of both the linings is described. This allows practitioners to evaluate and compare the effectiveness of both R/FRC and RC solutions after 20 years of service.

2 Assessment of the Linings

2.1 The Conceptual Design of the Structures

Tunnels are concrete infrastructures that typically require a minimal content of reinforcement, especially when constructed in zones with good geo-mechanical rock mass. Indeed, the surrounding ground provides uniform confinement and low acting loads; thus, low bending moments are present in the lining cross-sections, in which stress distribution remains fully compressive. Even when bending moments are present, the resulting tensile stresses do not lead to the use of extensive reinforcement.

As shown in Fig. 2, the behavior of slightly reinforced concrete beams in three-point bending can be reproduced in terms of the load-deflection curve (P-η), whose shape depends on the reinforcement ratio ρ (i.e., the ratio between the area of steel reinforcement A_s and that of concrete A_c). In particular, the increment of A_s, and ρ as well, has a limited impact on the effective cracking bending moment, $M_{cr}^{\star}$, as it is mainly influenced by the tensile capacity of concrete. On the contrary, the amount of reinforcement plays a crucial role on the ultimate bending moment M_u, which increases with the increment of A_s (and ρ).

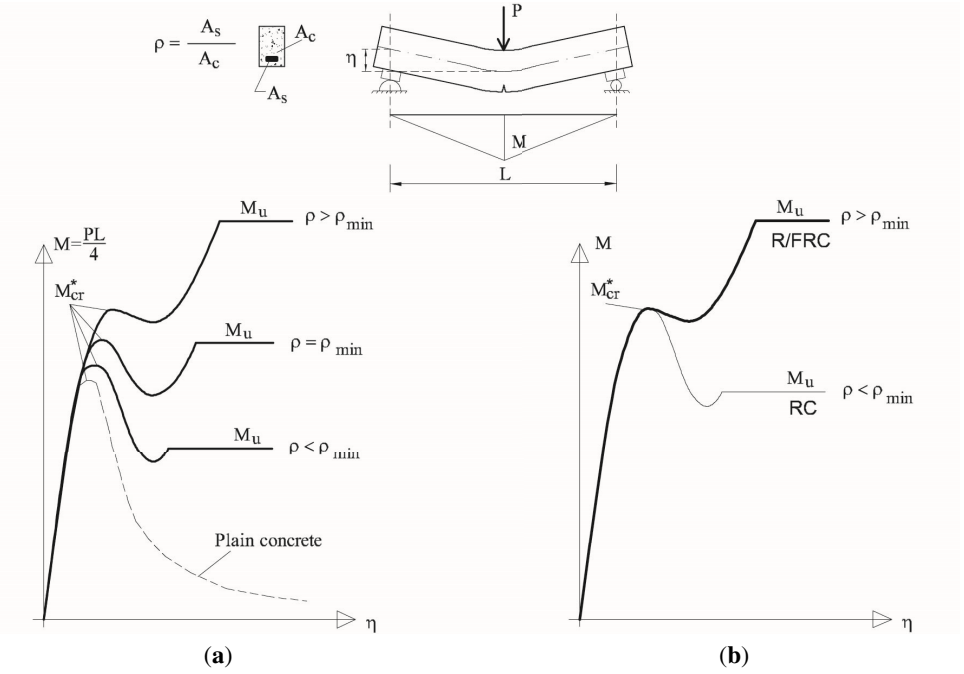

Figure 2: (**a**) M-η Relationships of RC beams tested in three-point bending; (**b**) Effect of fibers on the behavior of slightly reinforced concrete beams.

In general, a minimum reinforcement ratio ρ_{min} must be incorporated to avoid the brittle failure, which occurs when $M_{cr}^{\star} > M_u$ [8]. Thus, the acceptable content of reinforcement is reached when:

$$\rho \geq \rho_{min} \text{ or when } M \geq M^{*}_{cr} \quad (1)$$

Although the ITA-AITES WG2 guidelines [13] were originally developed focusing on precast segmental linings, the same performance-based design approach was applied to the conventional cast *in-situ* tunnel linings investigated herein. In particular, the content of reinforcement was optimized, by minimizing the amount of conventional steel rebar used to satisfy Eq. (1). Among the three strategies suggested by ITA-AITES WG2 and shown in Table 1, the hybrid solution was adopted. It consists of combining traditional rebar and steel fibers.

Table 1: ITA AiTES tunnel reinforcement types [13].

Section Type	Description	Condition of Use
RC	Conventional rebar only	High stress (Traditional Type)
FRC	Replace all traditional reinforcement with fibers	Low-Moderate stress zones
Hybrid (R/FRC)	Combine moderate fiber content with reduced bar reinforcement	High bending zones, seismic design, weak ground (Recommended Recently)

The hybrid R/FRC solution is particularly convenient when the content of rebar does not satisfy Eq. (1) (see Fig. 2b). As shown by the tests performed by Patty et al. [14], in this situation either the increment of A_s or the addition of a suitable amount of steel fibers can be sufficient to have an ultimate bending moment larger than the cracking moment. Similarly to the increment of A_s, the presence of fibers does not substantially modify $M_{cr}{}^{\star}$, but it remarkably increases M_u (Fig. 2).

Accordingly, a numerical procedure was introduced to calculate the minimum reinforcement of a hybrid R/FRC solution in the Tunnel #1 and Tunnel #2 [8]. This approach was based on the Wuczkowski method [15], which is generally used to calculate the amount of steel rebar in tension in RC cross-sections subjected to bending moments and normal actions. It consists of the following iterative procedure (Fig. 3):

- Input data: geometrical properties of the cross-section, material properties (see Table 2), elastic modulus of steel (assumed to be in the linear elastic regime), and the applied normal force N_d.
- Calculate the effective cracking moment $M^{\star}_{cr}$ with the linear elastic theory (the flexural strength f_{ctf} is computed from the class of concrete [16]).

According to the producer's data sheet, steel fibers were supplied in sheets with water-soluble glue. This glue prevented clamping during mixing and ensured a good distribution of the fibers throughout the concrete mixture.

- Translate N_d into the centroid of rebar in tension from the axis of the beam (Fig. 3a,b).
- Assume λ value (which is the strain in the axis of the beam—Fig. 3b).
- Compute the curvature μ of the cross-section by imposing the yielding of rebar in tension e_{syd}—Fig. 3b.
- When μ and λ are known, it is possible to compute the whole distribution of strain $e(y)$ (in Fig. 3b, where plane sections remain plane) and the stress profile s(e, y) (Fig. 3c).
- Compute the bending moment M_u with respect to the centroid of the steel in tension (equilibrium to rotation)
- If $M^{\star}_{cr} \neq M_u$, go back to step 5 with a new value of λ.

- When $M^{\star}_{cr}$ is numerically equal to M_u, A_{smin} can be evaluated by imposing the equilibrium to translation of the whole cross-section.

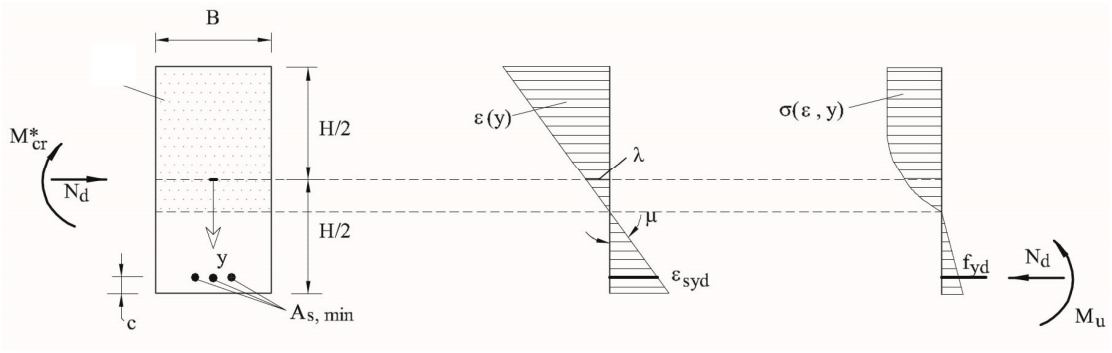

Figure 3: Computing the minimum reinforcement in R/FRC beams [8]: (**a**) geometrical properties of the beam (**b**) strain profile; (**c**) stress profile.

Table 2: Material properties.

Materials	Description
Concrete	Compressive strength C25/30
Rebar	Grade B500
FRC	Dramix 65/60 BG dosage of about 30–40 kg/m^3 Length 60 mm Diameter 0.95 mm Aspect ratio 65 Nominal Tensile Resistance 1160 (MPa) Young Modulus 200,000 (MPa)

As a result, only a limited amount of conventional reinforcement was required (see Fig. 4a), typically provided in the form of a lightweight, self-supporting mesh (see Fig. 4b). This mesh not only ensured the resistance to bending moment and crack control but also reduced the labor work of rebar placement and increased the speed of construction.

To adequately characterize the contribution of fibers to the mechanical performance of the concrete, and to demonstrate the theoretical aspects discussed above, experimental verification was carried out by means of three-point bending tests on notched FRC specimens. These tests were specifically intended to evaluate the quality of FRC by measuring the post-cracking behavior of small beams.

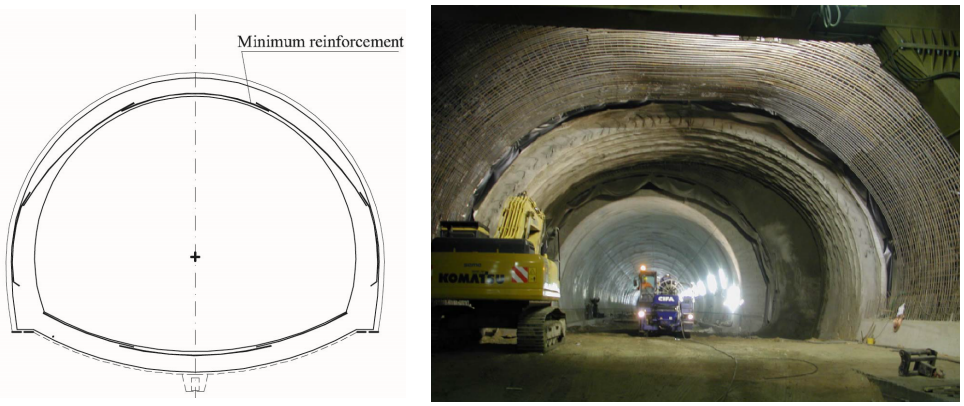

(**a**) (**b**)

Figure 4: (**a**) The minimum reinforcement in a tunnel cross-section; (**b**) the position of steel rebar in tunnels.

The results of these tests are summarized in Table 3, which reports the key mechanical parameters used to characterize FRC. In particular, $f_{ct,\,fl}$, represents the flexural tensile strength at first cracking, whereas parameters $f_{R,1}$ and $f_{R,4}$ are the residual flexural tensile strengths measured at specified crack mouth opening displacements. These values are directly related to the fiber bridging capacity during the post-cracking stage. In addition, the fracture energy G_F represents the energy dissipated during crack propagation, which is a direct indicator of the FRC toughness.

Table 3: 3-point bending test results summary obtained on notched beam specimens.

Materials	Tensile Resistance $f_{ct,fl}$ (MPa)	Residual Resistance $f_{R,1}$ (MPa)	Residual Resistance $f_{R,4}$ (MPa)	Fractural Energy G_F (N/mm)
Average Value	5.14	2.37	1.55	6.12
Mean square error	0.334	0.416	0.376	1.56
Characteristic Value	4.56	1.65	0.902	3.59

2.2 The Final Design of the Linings

The total length of the Tunnel #1 is 1042 m, whereas the Tunnel #2 is 660 m long. Both tunnels were constructed using traditional excavation methods, with cast-*in-situ* concrete lining. The internal radius of the tunnels is 6.3 m, with a cross-sectional excavation area ranging from 116 to 150 m^2. Three types of cross-sections were used in both the tunnels: in Tunnel #1, most of the cross-sections were made with plain (Fig. 5a) and traditionally reinforced (Fig. 5b) concrete, whereas the R/FRC cross-sections (Fig. 5c) were adopted in Tunnel #2. Finally, at the interface with rocks, the concrete was protected (impermeabilized) with Polyvinyl Chloride (PVC) and double Non-Woven Geotextile Protection (TNT) layers.

The Tunnel #1 has a relatively uniform longitudinal profile. The tunnel linings consist of 87 panels (including four artificial panels at both entrances), having a length of 12 m each, as illustrated in Fig. 6. The same figure also shows the type of cross-sections (Fig. 5) with different colors along the longitudinal profile. They were designed in accordance with the approach described in the previous sections. After evaluating the effect of loads, i.e., the bending moment and normal action M_{Ed}-N_{Ed} in each cross-section of the panel, the

interaction domain M_{Rd}-N_{Rd} of plain concrete was computed. With respect to M_{Rd}-N_{Rd} of plain concrete, the values of M_{Ed}-N_{Ed} determine three situations:

1. If M_{Ed}-N_{Ed} is inside the domain M_{Rd}-N_{Rd} of plain concrete, no reinforcement was introduced, and only the plain cross-sections (Fig. 5a) were adopted (green zones in Fig. 6a)
2. If M_{Ed}-N_{Ed} is outside the domain M_{Rd}-N_{Rd} of plain concrete, and far from its border, only steel bars were used to reinforce the cross-sections (Fig. 5b). These cross-sections are colored red in Fig. 6a.
3. If M_{Ed}-N_{Ed} is outside the domain M_{Rd}-N_{Rd} of plain concrete, but close to the border, a combination of steel fibers and a minimum amount of steel bars was used to reinforce the cross-sections (Fig. 5c). These parts of the lining correspond to zones colored in blue in Fig. 6a.

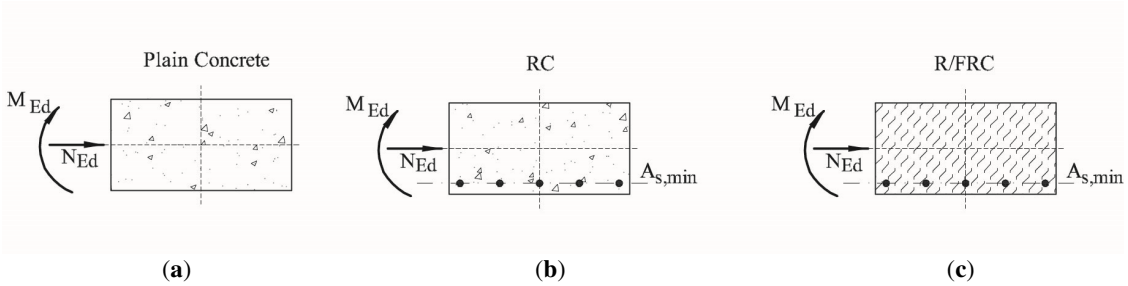

Figure 5: The resisting cross-section of the tunnels: (**a**) Plain concrete; (**b**) RC; (**c**) R/FRC.

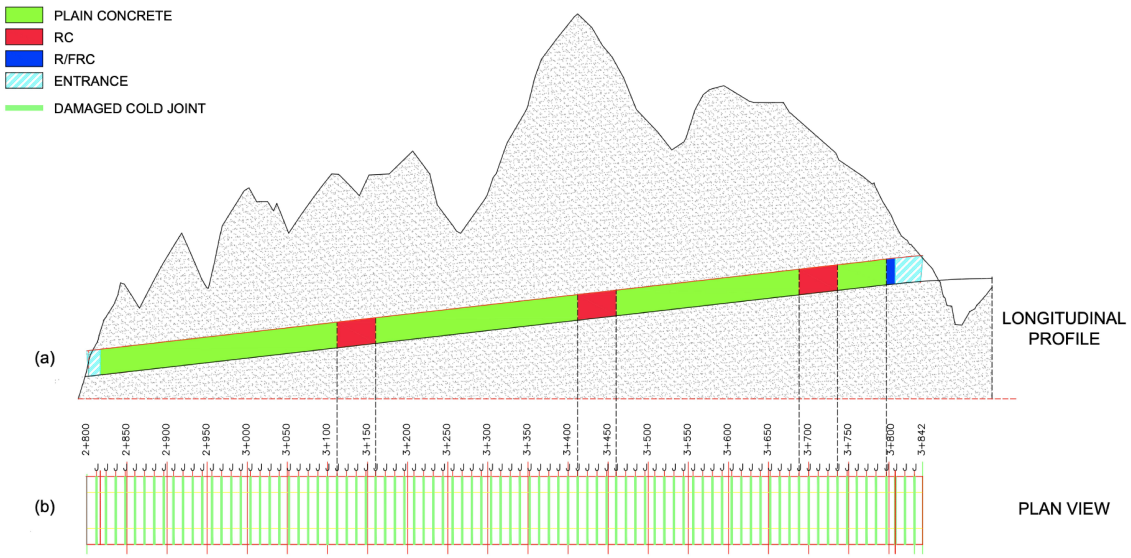

Figure 6: Tunnel #1: (**a**) longitudinal profile with the type of resisting cross-section; (**b**) plan view of the panels with the cold joints.

As shown in Fig. 6, a plain concrete cross-section with no traditional reinforcement was adopted for most of the tunnel due to the low stresses acting on the lining and to the high-quality of soil surrounding it. The zones with high bending moments or localized tensile stresses, and with the necessity of using only conventional steel bars, are limited to 15% of the lining. Hybrid R/FRC was used in only 1% of the whole lining (blue zones).

The longitudinal profile of Tunnel #2, depicted in Fig. 7, is composed of 55 panels (including four artificial panels at both entrances), with a length of 12 m each. They were designed with the same methodology used in Tunnel #1. As a result, in most of the lining, blue zones with hybrid R/FRC cross-sections (Fig. 5c) are predominant. Only 20% of the lining included only steel rebar (red zones in Fig. 7a), whereas in Tunnel #2, there are no cross-sections without reinforcement. This is due to the change of ground conditions and structural demands as well, with respect to Tunnel #1. The hybrid strategy was successfully implemented in Tunnel #2 because it allowed the reduction of material usage, incorporating minimal steel mesh reinforcement (Fig. 4). In addition to the direct reduction of the overall rebar weight and of cost, this methodology also minimized the time for casting the panels.

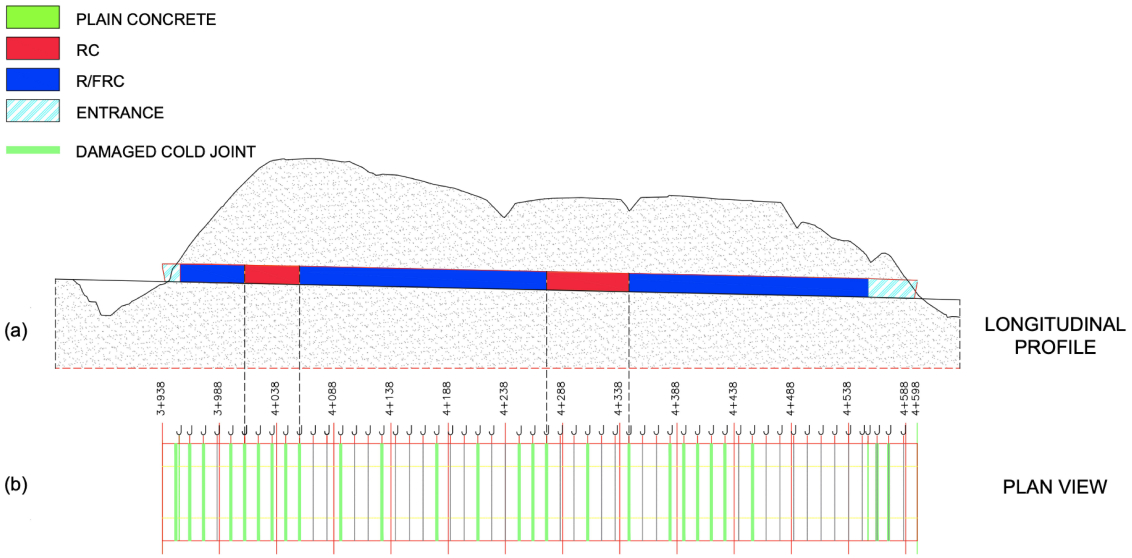

Figure 7: Tunnel #2: (**a**) longitudinal profile with the type of resisting cross-section; (**b**) plan view of the panels with the cold joints.

As mentioned above, Tunnel #2 is characterized by heavier local ground conditions, more demanding soil characteristics, and higher loading requirements than Tunnel #1. As illustrated in Section 2.2, these unfavorable conditions led to increased internal forces, bending moments, and tensile stresses in the lining. In order to adequately account for these higher stress demands and to enhance the post-cracking behavior of the concrete sections, fiber-reinforced concrete (FRC) was intentionally adopted in Tunnel #2. The use of FRC was therefore a design-driven choice aimed at improving crack control, stress redistribution, and overall structural robustness under elevated loading conditions, rather than a secondary or incidental material variation. Due to the presence of fibers, the effects of unpredictable events, like the spalling in the cold joints, are effectively mitigated.

Concerning the environmental exposure, Tables 4 and 5 summarize the temperature and relative humidity variations recorded at the tunnel site over the last five years (2021–2025). Although these data do not cover the entire service life of the tunnels, they give information on the environmental conditions of the tunnels. No other data, including freezing-thawing and periodical maintenance, are available.

The temperature data indicate pronounced annual thermal variability, with minimum values consistently below 0°C and maximum values exceeding 30°C. As a result, the temperature varies approximately 38°C–41°C yearly. Such fluctuations are known to induce cyclic thermal expansion and contraction of the

concrete, particularly at cold joints of the linings. Over time, thermal stresses and movements may lead to cracking and localized spalling, especially when joint construction detailing is not adequate.

Table 4: Annual temperature statistics at the tunnel site over the period 2021–2025.

Year	Average	MIN	MAX	Difference
2021	12.91	−5.6	32.3	37.9
2022	13.99	−6.2	35.2	41.4
2023	13.90	−4.3	34.1	38.4
2024	13.78	−4.2	33.7	37.9
2025	14.03	−4.3	34.8	39.1

Table 5: Annual relative humidity statistics at the tunnel site over the period 2021–2025.

Year	Average	MIN	MAX	Difference
2021	70.62	15.0	98.5	83.5
2022	67.67	8.8	98.3	89.5
2023	69.76	6.0	95.0	89.0
2024	73.60	12.7	96.5	83.8
2025	72.58	18.6	97.0	78.4

Additionally, the relative humidity data further highlight high moisture variability, with maximum values approaching saturation (100%) and minimum values occasionally below 10%. These conditions are particularly relevant for tunnel durability, as they promote moisture ingress through cracked or imperfectly sealed joints. In the two tunnels, several instances of water intrusion at construction joints were observed during visual inspections, especially in Tunnel #1 constructed without fiber-reinforced concrete. The presence of water at cracked joints accelerates damage mechanisms, such as freeze–thaw action, localized deterioration, and progressive spalling. On the contrary, Tunnel #2, where fiber-reinforced concrete was implemented, generally shows reduced damage at joint locations, with fewer cases of spalling and less evidence of water penetration.

2.3 Inspection and Damage Assessment of the Tunnels after 20 Years in-Service

After two decades of being in service, both tunnels were inspected with extensive destructive tests to assess the current conditions. Core samples were extracted from the concrete linings to measure the depth of carbonation and the compressive strength. The main objective of the destructive tests, following the procedures prescribed in EN 12390-3:2019 [17] and EU 14630:2006 [18], was to determine both the dept of carbonation and concrete strength. Additionally, a general visual inspection was held to check the current situation and to provide a qualitative evaluation of the durability of the structure. Table 6 reports the results of the destructive tests.

The measurement of compressive strength is reported primarily to verify that the *in-situ* concrete quality remains consistent with the original design requirements, and no significant mechanical degradation has occurred over the service life of the tunnels. Similarly, the carbonation depths are consistently lower than the thickness of concrete cover, indicating that reinforcement corrosion is not affecting the durability of either of the tunnels.

Table 6: Results of the tests on concrete cores drilled from the linings.

Tunnel	Core ID	Carbonation Depth [mm]	Compressive Strength [MPa]
Tunnel #1	C-C1	40	36.4
	C-C2	15	57.2
	C-C3	15	30.2
	C-C4	0	40.8
	C-C5	20	14
	C-C6	20	43.8
	C-C7	20	38.9
	C-C8	20	35
	C-C9	30	37.2
	C-C10	20	55.2
	C-C11	20	41.7
	C-C12	15	59.6
	C-C13	0	53.9
	C-C14	10	54.5
	C-C15	25	49.6
	Average	**18**	**43.2**
Tunnel #2	T-C1	40	43.0
	T-C2	15	51.9
	T-C3	15	36.6
	T-C4	0	44.0
	T-C5	20	35.7
	T-C6	20	52.6
	T-C7	20	53.5
	T-C8	20	58.9
	T-C9	30	36.0
	T-C10	20	60.9
	Average	**20**	**47.3**

A statistical analysis was performed for the results of compressive strength concerning Tunnel #1 and Tunnel #2. If a normal distribution of the values is assumed, the resulting distributions show a general agreement with the experimental data of compressive strength. Concrete, drilled from random parts, has a compressive strength consistently exceeding the initial design class (C25/30), with an average value of about 45.0 MPa for both tunnels (see Figs. 8a and 9a). In the case of Tunnel #1, the strength of one core (C-C5) falls below the 5th percentile of the fitted distribution. Thus, it can be considered as a statistical outlier.

In parallel, the measurements of carbonation depth are illustrated in Figs. 8b and 9b for Tunnel #1 and Tunnel #2, respectively. In all the cores, the carbonation depths remain below the thickness of concrete cover (50 mm), confirming that the protective function of concrete is still effective. Despite the long service life, both RC and FRC cross-sections of the tunnels have been performing well, without any significant corrosion of steel.

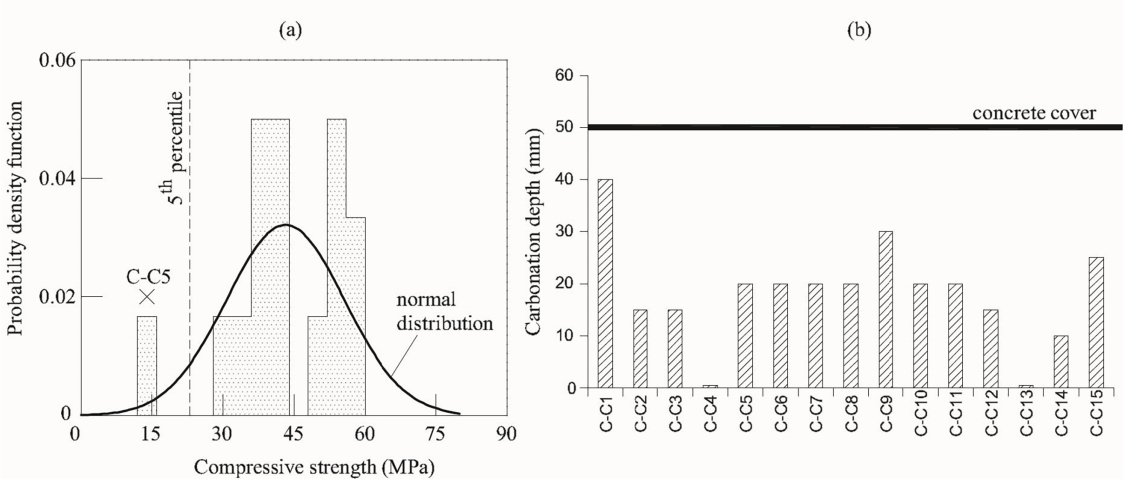

Figure 8: Graphical representation of the concrete tests—Tunnel #1 (**a**) compressive tests; (**b**) carbonation depth.

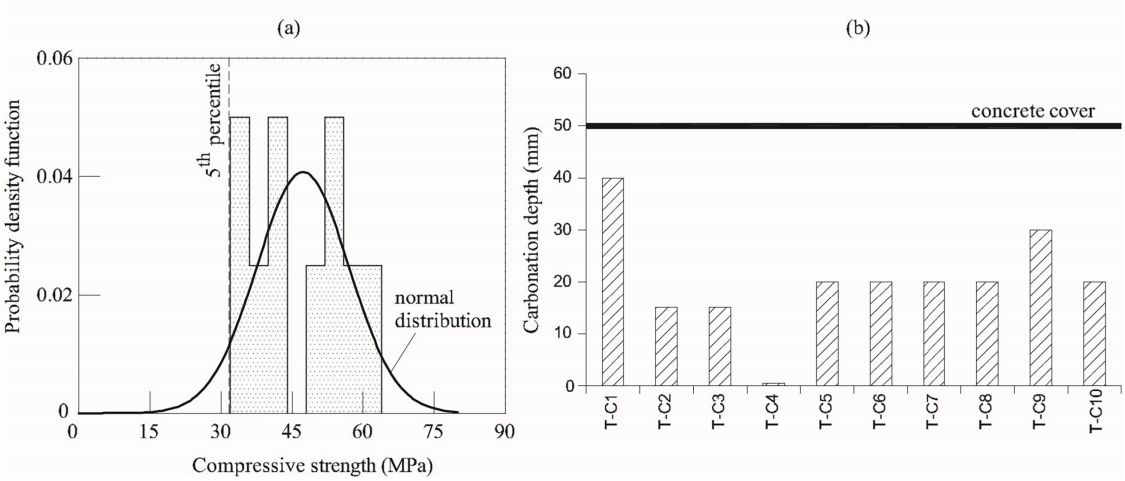

Figure 9: Graphical Representation of the concrete tests—Tunnel #2 (**a**) compressive tests; (**b**) carbonation depth.

However, cracks and the spalling phenomenon, with an extensive detachment of concrete materials, were noticed remarkably. This type of local failure is visible in the inner face of the linings around joints of the panels. In Tunnel #1, made with only conventional plain concrete with and without rebar, the spalling phenomenon was noticed in all the joints of the tunnel. Based on the measurements of compressive strength and carbonation depth, the observed deterioration cannot be attributed to insufficient concrete strength or corrosion-induced damage mechanisms. Indeed, the lack of durability is predominantly associated with localized spalling at cold joints, which in turn is driven by stress concentrations and restrained deformations.

As shown in Tables 7 and 8, the detached fragments of concrete have different dimensions, not always representing a dangerous environment. For this reason, three levels of damage (Severe, High, and Minor), the location (sidewall, shoulder, and crown) of the spalled material, and the total length of the damaged joints have been used to quantify the magnitude of the failure. Although the environmental conditions are the same, a different level of damage is clearly visible in the two tunnels. Indeed, damaged cold joints are more vulnerable to water intrusion through the spalled parts.

Table 7: Spalling of concrete in the joints of Tunnel #1.

Location	Pictures	Sequence ID Number of Failed Joints	Length of Damage
Side wall		Severe Damage/Detachment: 7, 11, 12, 13, 14, 15, 19, 27, 32, 48, 49, 57, 75, 77, 78, 79, 81, 86, 88	33
		High Damage: 17, 40, 49, 72	90
		Minor Damage: 42, 54, 62, 66, 74, 82	22
Shoulder		Severe Damage: 14, 32, 57, 74, 77, 79, 81, 82, 86	72
		High Damage: 17, 27, 40, 72, 78	84
		Minor Damage: 42, 47, 54, 62, 66	62
Crown		Severe Damage: 9, 36, 49, 53, 55, 72, 86	50
		High Damage: 17, 19, 27, 40, 57, 67, 68, 71, 73, 78	76
		Minor Damage: 25, 33, 47, 54, 62, 66, 74, 76, 77, 81, 82, 83, 87	42

Table 8: Spalling of concrete in the joints of Tunnel #2.

Location	Pictures	Sequence ID Number of Failed Joints	Length of Damage
Side wall		Severe Damage: 7, 30	13
		High Damage:	–
		Minor Damage:	–
Shoulder		Severe Damage: 7, 35, 36	13
		High Damage:	–
		Minor Damage:	–

(Continued)

Table 8 (continued)

Location	Pictures	Sequence ID Number of Failed Joints	Length of Damage
Crown		Severe Damage:	–
		High Damage: 14	4
		Minor Damage: 5, 6, 7, 8, 33, 56, 58, 59	28

In Tunnel #2, the situation was better than in Tunnel #1, as spalling was detected only in some joints. Due to the presence of fibers, visible in Table 8, the integrity of the joint was mainly preserved, and only a few small concrete particles fell. Thus, steel fibers provided a significant contribution in reducing the damage of the joint, minimizing the dimensions of the spalled parts.

The different damage observed in both the tunnels is also illustrated in Figs. 6b and 7b, respectively, where the damaged joints between the panels are marked with a green line. In Tunnel #1, all the joints suffered heavy damage, whereas in Tunnel #2, spalling generally occurred in RC cross-sections rather than in the R/FRC panels.

3 Analysis of the Current Situation and Interventions

3.1 The Causes of the Spalling and Possible Mitigation

In massive structures, expansion and contraction joints are necessary. However, transverse joints are normally not needed in cast-*in-situ* concrete lining, as also suggested by ACI 224.3R-95 [19]. Indeed, the thermal expansions and contractions are remarkably lower than those of the concrete pavements or bridges, as the daily or seasonal variation of temperature is minimal, except at the entrances. Nevertheless, transversal joints are present because of the construction procedure, which is generally based on the use of formwork with a maximum length of 12 m (which is exactly the length of the panels in both the tunnels). Moreover, the presence of joints can also mitigate shrinkage cracking.

In the cases investigated herein, the transversal joints were not realized according to the standard methods (i.e., forming, tooling, sawing, and placement), as those shown in Fig. 10a [19]. On the contrary, new concrete was just cast adjacent to the previous panel, one or two days later (Fig. 10b).

Thus, the transversal joints of both the tunnels can be considered neither as expansion nor contraction joints, but cold joints. They were not properly detailed, as shown in Fig. 10a, and became favorable locations for temperature and stress concentration. In other words, they are not working to mitigate the effects of temperature; on the contrary, they are prone to spall, especially in plain concrete panels.

Although the fibers added in the case of Tunnel #2 have proven a sort of mitigation against spalling, studies concerning the behavior of FRC around concrete joints are scarce. However, in other situations, such as Alkali-Silica Reaction (ASR), corrosion, and sudden impact, the current literature provides several research projects on the spalling mitigation due to the presence of a fiber-reinforcement. Indeed, ASR is an internal expansive reaction between the reactive silica of some aggregates and the alkalis of the cement mixture. As concrete tends to increase in volume, microcracks and concrete spalling are generally observed [20]. Adding fibers is not a preventive action to eliminate this chemical reaction, but it reduces the microcrack propagation and widening, limiting the connectivity of ASR gel paths and reducing the expansive effects.

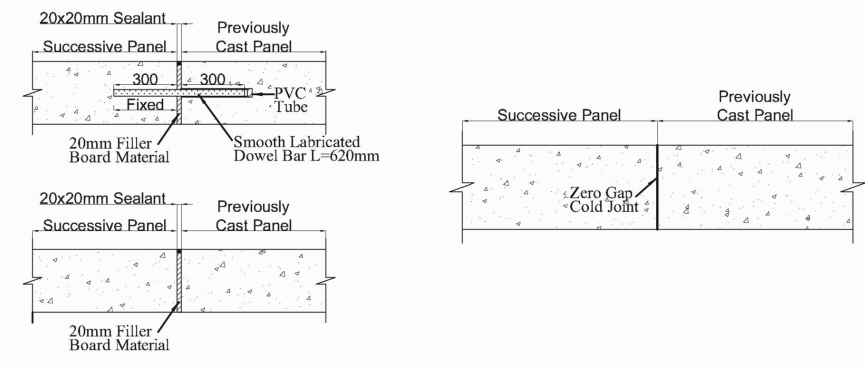

Figure 10: Typical joints of concrete structures: (**a**) expansion joint details with and without dowel bars [19]; (**b**) cold joints in the Tunnel #1 and Tunnel #2.

In the same way, when intensive chloride mediums and carbonation foster the corrosion of rebar, a chemical reaction leads to rust in steel and results in a relatively great increment in volume. Using fibers becomes beneficial in terms of bridging the microcracks at early stages and preventing them from propagating until complete failure or spalling [21]. Also, concrete has a brittle failure against mechanical shock or a sudden impact, such as a car accident in tunnels. In the presence of fibers, concrete energy can be absorbed and shows an acceptable residual capacity compared to the pre-impact concrete element state [22]. Thanks to a high bridging capability, fibers convert the brittle fracturing of particles into progressive energy dissipation [23].

The beneficial effects of steel fibers on concrete durability could explain how FRC structures can reduce damage and continue their function safely, even in unforeseen situations, like the presence of cold joints in the two tunnels investigated herein. Thus, R/FRC linings are resilient structures [24]. In Tunnel #2, the inclusion of fibers in concrete mixtures made the lining more resilient than that of the plain concrete lining of Tunnel #1. Fibers increased the structure's damage tolerance, leading to the detachment of only small concrete particles (see Table 7), thus preserving the original state of the structure. On the contrary, large particles were detached from the cold joints of Tunnel #1 lining (see Table 6). Accordingly, the addition of fibers into concrete mixtures has enhanced the toughness of concrete in tension not only in the cross-sections of the panels, but also locally in the cold joints.

3.2 Interventions

Considering the situation of all the joints in both the tunnels (Figs. 6b and 7b), interventions on those damaged by concrete spalling are needed. Specifically, the repair technique consists of bonding a new concrete layer, containing a steel mesh, in the intrados of the existing lining and anchoring it to the inner part of the structures.

In 2016, a trial application of the polyurea resin spraying method was carried out in Japan, where spalling and water intrusions had been detected not only at the joints, but also within the panels of a concrete lining. Polyurea resin was applied after spraying a primer to increase adhesion between the concrete surfaces and the resin, particularly in areas affected by water intrusion and seepage [25]. In the case of Tunnels #1 and #2, such a repairing solution was not applied for two main reasons. First of all, both primer and Polyurea resin were not available in Italy. In addition, as no structural calculations were needed, practitioners selected a repair solution provided by a local chemical company in the building sector. As shown in Fig. 11a, the restoration work on the damaged joints consists of the following steps:

- Scarify the concrete surface around the joint.
- Apply a cement-based mortar with the shotcrete to restore the section, after anchoring the existing reinforcement with Ø14 grouted bars.
- Apply a lightweight protective mesh made of stainless steel Ø1.6 mm (mesh size 12.7 mm × 12.7 mm) and a welded stainless-steel mesh Ø 5 mm (mesh size 50 mm^2 × 50 mm^2) over a width of 1 m across the joint.
- Anchor the mesh with stainless steel chemical anchors (see Fig. 11b).

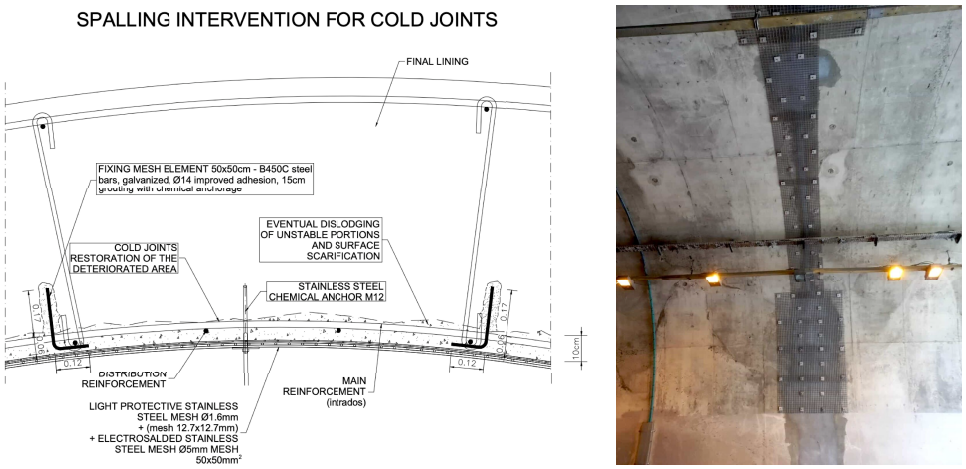

(**a**) (**b**)

Figure 11: Repairing cold joints of tunnel linings: (**a**) Detail of the restoration works; (**b**) On site application of the repairing system.

As illustrated in Table 9, the cost of intervention on a single joint was the same in both the tunnels. However, the number of damaged joints in the lining of Tunnel #2 was remarkably lower. This was not only due to the shorter length of the tunnel, but also to the presence of FRC. Indeed, the cost of intervention per unit length of Tunnel #1 was more than twice that of Tunnel #2. This is a further confirmation of the resilience of FRC lining: the higher the toughness of cement-based concrete, the higher the capability of absorbing the extra stresses, like those of cold joints, and enhancing the durability of structures. Hence, the cost of maintenance is reduced as well.

Table 9: Cost of reparation interventions in the two tunnels.

Tunnel	Cost of One Interevent [€]	Length of the Tunnel [m]	Number of Retrofitted Joints	Total Cost of Interventions [€]	Cost of Interventions Per Unit Length of Tunnel Lining [€/m]
Tunnel #1	3520	1042	86	302,720	291
Tunnel #2		660	26	91,520	137

It must be remarked that the previous economic analysis focuses only on the restoration following failure, without delving deeply into a quantitative analysis of the indirect costs, including those related to

road closure. Nevertheless, as the use of FRC tends to reduce the number of damaged joints, the duration of retrofitting activities is minimized, thereby minimizing the indirect costs due to the nonuse of the tunnels.

4 Conclusions

According to the results of a survey on two existing concrete linings, the following conclusions can be drawn:

- The combination of a small amount of reinforcing bars and a fiber-reinforcement is a valid alternative to traditional reinforced concrete lining, as demonstrated by Tunnel #2, which has been in service for more than 20 years.
- Both plain concrete and FRC used in the two tunnels have demonstrated the capability of maintaining the mechanical properties, such as compressive strength, and of protecting the integrity of steel rebar over the years.
- Moreover, the use of a fiber-reinforcement renders concrete structure more resilient, and capable of facing unforeseen actions. Indeed, the presence of fibers significantly reduced the damage to the cold joints of Tunnel #2, compared to the heavy spalling observed in plain concrete joints of Tunnel #1.
- FRC used in tunnels leads to a reduced maintenance of lining, cutting the unit cost of restoration interventions. Indeed, the cost of repairing cold joints in Tunnel #1 was twice that of Tunnel #2.

As long-term field observation has revealed further advantages of using FRC in structural applications, new studies must be devoted to the structural analysis of cold joints. In particular, the relationship between the class of FRC and the degree of spalling phenomenon has to be analytically quantified.

Acknowledgement: The present study has been developed within the National project AID-STRU—AgeIng and Degradation in the performances of STRUctures: model- and data-driven tools embedded in digital-twins (PRIN 2022).

Funding Statement: The authors received no specific funding for this study.

Author Contributions: Study conception and design: Alessandro P. Fantilli, Bernardino Chiaia; Data collection: Mustapha Hatoum, Georgios Kalamaras; Analysis and interpretation of results: Mustapha Hatoum, Alessandro P. Fantilli; Draft manuscript preparation: Mustapha Hatoum, Alessandro P. Fantilli, Georgios Kalamaras; All authors reviewed and approved the final version of the manuscript.

Availability of Data and Materials: Data available on request from the authors. The data that support the findings of this study are available from the corresponding author, Alessandro P. Fantilli, upon reasonable request.

Ethics Approval: Not applicable.

Conflicts of Interest: The authors declare no conflicts of interest.

References

1. Li Y, Ruan X, Zhang T, Fu B, Zeng H. Durability design and construction enhancing of concrete structures in mesoscopic approach: a case study of a large-scale anchorage structure. Case Stud Constr Mater. 2023;19(1):e02404. doi:10.1016/j.cscm.2023.e02404.
2. Peng K, Yi G, Wang Y, Luo S, Wu H. Experimental and theoretical analysis of spalling in deep hard rock tunnels with different arch structures. Theor Appl Fract Mech. 2023;127(7):104054. doi:10.1016/j.tafmec.2023.104054.
3. Xu Q, Xie J, Zhou F, Tang Z. Numerical simulation and analysis of the causes and distribution of secondary lining cracks in overlapping railway tunnels. Appl Sci. 2023;13(11):6436. doi:10.3390/app13116436.
4. Bi J, Jiang H. Water infiltration in drained circular tunnels: an analytical solution and its simplification. Géotechnique. 2025;75(2):180–91. doi:10.1680/jgeot.23.00040.

5. Fromsa A, Ararsa W, Quezon ET. Effects of poor workmanship on building construction and its implication to project management practice: a case study in Addis Ababa City. J Xidian Univ. 2020;14(9):1174–88. doi:10.31224/osf.io/kbnau.
6. Tsuno K, Kishida K. Evaluation of spalling of concrete pieces from tunnel lining employing joint shear model. Tunn Undergr Space Technol. 2020;103(6):103456. doi:10.1016/j.tust.2020.103456.
7. Meguid MA, Dang HK. The effect of erosion voids on existing tunnel linings. Tunn Undergr Space Technol. 2009;24(3):278–86. doi:10.1016/j.tust.2008.09.002.
8. Chiaia B, Fantilli AP, Vallini P. Evaluation of minimum reinforcement ratio in FRC members and application to tunnel linings. Mater Struct. 2007;40(6):593–604. doi:10.1617/s11527-006-9166-0.
9. Liao L, de la Fuente A, Cavalaro S, Aguado A. Design of FRC tunnel segments considering the ductility requirements of the Model Code 2010. Tunn Undergr Space Technol. 2015;47(6):200–10. doi:10.1016/j.tust.2015.01.006.
10. Mohammad Hosseini S, Mousa S, Mohamed HM, Ferrier E, Benmokrane B. Experimental and analytical investigation of precast fiber-reinforced concrete (FRC) tunnel lining segments reinforced with glass-FRP bars. Tunn Undergr Space Technol. 2023;139(5):105230. doi:10.1016/j.tust.2023.105230.
11. Qian S, Li VC. Influence of concrete material ductility on headed anchor pullout performance. ACI Mater J. 2009;106(1):72–81. doi:10.14359/56319.
12. Granju JL, Ullah Balouch S. Corrosion of steel fibre reinforced concrete from the cracks. Cem Concr Res. 2005;35(3):572–7. doi:10.1016/j.cemconres.2004.06.032.
13. Bakhshi M, Nasri V, Chiriotti E, Tluczek R. Guidelines for the design of segmental tunnel linings. Genève, Switzerland: ITA-AITES; 2019. 60 p.
14. Patty AH, Sonny Yoedono B, Sunik S. A study on toughness contribution to structural capacity of reinforced concrete beam. In: Reinforced concrete structures—innovations in materials, design and analysis. London, UK: IntechOpen; 2023. doi:10.5772/intechopen.1001442.
15. Walther R, Miehlbradt M. Dimensionnement des structures en béton: bases et technologie. Lausanne, Switzerland: Presses Politechniques Universitaires Romandes; 1990. (In French).
16. EN 1992-1-1. Eurocode 2: design of concrete structures-part I: general rules and rules for buildings. Brussels, Belgium: European Committee for Standardization; 2002.
17. BS EN 12390-3:2019. Testing hardened concrete—compressive strength of test specimens. London, UK: British Standards Institution; 2019.
18. EN 14630:2006. Products and systems for the protection and repair of concrete structures—test methods—determination of carbonation depth in hardened concrete by the phenolphthalein method. London, UK: British Standards Institution; 2006.
19. ACI Committee 224. 224.3R-95: joints in concrete construction (Reapproved 2008) [Internet]. 1998 [cited 2025 Feb 5]. Available from: https://www.concrete.org/publications/internationalconcreteabstractsportal/m/details/id/5113.
20. Giaccio G, Bossio ME, Torrijos MC, Zerbino R. Contribution of fiber reinforcement in concrete affected by alkali-silica reaction. Cem Concr Res. 2015;67(3):310–7. doi:10.1016/j.cemconres.2014.10.016.
21. Marcos-Meson V, Michel A, Solgaard A, Fischer G, Edvardsen C, Skovhus TL. Corrosion resistance of steel fibre reinforced concrete—a literature review. Cem Concr Res. 2018;103:1–20. doi:10.1016/j.cemconres.2017.05.016.
22. Vairagade VS, Dhale SA. Impact resistance of hybrid steel fiber reinforced concrete. Hybrid Adv. 2023;3:100048. doi:10.1016/j.hybadv.2023.100048.
23. Zhang P, Kang L, Wang J, Guo J, Hu S, Ling Y. Mechanical properties and explosive spalling behavior of steel-fiber-reinforced concrete exposed to high temperature—a review. Appl Sci. 2020;10(7):2324. doi:10.3390/app10072324.
24. Brefo JA, Yakin Z. The role of fiber-reinforced and self-healing concrete in enhancing U. S. infrastructure durability. Eng Sci Technol J. 2025;6(5):216–29. doi:10.51594/estj.v6i5.1938.
25. Oe A, Shimamoto K, Ushida T, Suzuki M, Yashiro K, Miyata Y, et al. Method for preventing spalling of tunnel lining with polyurea resin: application to seepage area and uneven area. In: Tunnelling into a sustainable future—methods and technologies. London, UK: CRC Press; 2025. p. 4257–64. doi:10.1201/9781003559047-542.